a high ratio of PEI:Cu^{2+} (>20) show EPR spectra of $Cu(PEI)_4^{2+}$ or $Cu(PEI)_5^{2+}$ complexes (depending on the pH value) in which the anisotropic features are very prominent due to the slow tumbling rate of the macromolecules. This kind of spectra exhibiting copper hyperfine structure is a direct confirmation of the binding of Cu^{2+} to the polymer. Solutions containing PEI, which is more loaded with Cu^{2+} (PEI:Cu^{2+} < 10), yield isotropic broaden line spectra due to the exchange interaction between the paramagnetic centers (Figure 4, n = 2, 3), even if the total concentration of Cu^{2+} is low. Indeed, with increasing Cu^{2+} concentration the number of "free" nitrogen sites available for coordination diminishes, and Cu^{2+} ions are constrained to occupy neighboring positions in the polymer coil. The phenomenon of exchange Cu^{2+}–Cu^{2+} interactions has been called the "clothes-line" effect.[5] A further decrease of the PEI:Cu^{2+} ratio (≤5) yields spectra in which the signals of Cu^{2+}(aq) and of Cu^{2+} bound to PEI are clearly discernible (Figure 4, n = 4, 5). The appearance of the signal corresponding to the formation of Cu^{2+}(aq) species shows that the polymer is completely loaded with Cu^{2+} ions, and consequently no more "free" nitrogen sites are available for coordination.

Figure 5 shows an analogous series of spectra of PEI loaded partially with Pt^{2+} (PEI:Pt^{2+} = 16). As expected, the "clothes-line" effect is enhanced at comparable concentration ratios as compared to "free" PEI. Exchange interactions are already clearly observed in a solution containing PEI:Pt^{2+}:Cu^{2+} = 16:1:1 (Figure 5, n = 1), and the relative concentration of the Cu^{2+}(aq) is larger in the solution containing 16 PEI:1 Pt^{2+}:4 Cu^{2+} (Figure 5, n = 4), as compared to 16 PEI:4 Cu^{2+} (Figure 4, n = 4), indicating a significantly reduced capacity for Cu^{2+} binding of the Pt(II)-loaded PEI. These effects are strongly enhanced in a solution containing PEI:Pt^{2+} = 8 (Figure 6). Cu^{2+}(aq) is already clearly present in a solution containing PEI:Pt^{2+}:Cu^{2+} = 8:1:0.5.

The spectra of solutions containing the $Pt(bpy)(PEI)_2^{2+}$ (PEI:Pt^{2+} = 16, 8) show a similar evolution with the increase of Cu^{2+} concentration, as the ones of $Pt(PEI)_4^{2+}$.

Spectra in frozen solution are anisotropic only for low Cu^{2+} concentrations, with g_1 = 2.21, g_2 = 2.09, and $A = 74 \times 10^{-4}$ cm^{-1}; while they become isotropic (g_{iso} = 2.10) in solutions with a high content of Cu^{2+}. The line widths in the isotropic spectra were measured from peak to peak. It was found that they narrow with the concentration of Cu^{2+} until saturation of the polymer, and then there is a line broadening for solutions which have "overloaded" PEI. The diminution in the line widths is probably due to the "exchange narrowing" effect observed in concentrated solutions.[41]

Acknowledgment. This work was supported by the Swiss National Science Foundation. We are very thankful to Felix Fehr for carrying out ^{195}Pt and ^{14}N NMR measurements and to C. W. Schläpfer for valuable discussions.

Registry No. $K_2[PtCl_4]$, 10025-99-7; *cis*-$Pt(NH_3)_2Cl_2$, 15663-27-1; $Pt(en)Cl_2$, 14096-51-6; $Pt(bpy)Cl_2$, 13965-31-6.

(41) McGarvey, B. R. *J. Phys. Chem.* **1957**, *61*, 1232.

Contribution from the Department of Chemistry, University of Houston, Houston, Texas 77204-5641, and Dipartimento di Scienze e Tecnologie Chimiche, Università di Roma Tor Vergata, 00173 Roma, Italy

Electrochemistry of Rhodium and Cobalt Corroles. Characterization of (OMC)Rh(PPh_3) and (OMC)Co(PPh_3) Where OMC is the Trianion of 2,3,7,8,12,13,17,18-Octamethylcorrole

K. M. Kadish,*,† W. Koh,† P. Tagliatesta,†,‡ D. Sazou,† R. Paolesse,‡ S. Licoccia,‡ and T. Boschi*,‡

Received December 10, 1991

The first oxidative electrochemistry of rhodium(III) and cobalt(III) corroles is reported in tetrahydrofuran, *N*,*N*-dimethylformamide, benzonitrile, and dichloromethane containing tetrabutylammonium perchlorate as supporting electrolyte. The investigated compounds are represented as (OMC)Rh(PPh_3) and (OMC)Co(PPh_3) where OMC is the trianion of 2,3,7,8,12,13,17,18-octamethylcorrole. Each complex undergoes up to three oxidations and two reductions depending upon solvent. The oxidations occur at the corrole π-ring system while the reductions occur at the rhodium or cobalt metal center. The three one-electron oxidations are electrochemically reversible by cyclic voltammetry at fast potential scan rates, but several chemical reactions occur at lower scan rates or in the presence of added triphenylphosphine. An overall oxidation reduction mechanism is proposed for each complex and comparisons are made with the well-characterized reactions of cobalt and rhodium tetraphenylporphyrins under the same experimental conditions.

Introduction

The electrochemistry of numerous metalloporphyrins has been reported under various solution conditions.[1] Complexes with 55 different elements have been characterized, and the use of these compounds in a variety of applications is well documented in the literature.[2,3] A number of porphyrin-like derivatives have also been studied. One such set of compounds are the corroles, which have a highly conjugated π electron system[4-7] but differ from the porphyrins in that they have a direct linkage between two pyrrole rings of the macrocycle. This structural difference gives rise to a deformation of the ligand so that none of the pyrrole rings can be completely in the same plane of the macrocycle.[8,9] Despite the fact that the corrole cavity is much smaller than that of porphyrins, the system is rather flexible and can accommodate large metal ions without substantial distortion of the macrocycle plane.[9] In the case of cobalt corroles, for which a crystal structure has been reported, the average Co–N distance is 1.87 Å.[10] This is analogous to the corresponding distance in cobalt complexes

† University of Houston.
‡ Università di Roma Tor Vergata.

(1) Kadish, K. M. *Prog. Inorg. Chem.* **1986**, *34*, 435.
(2) See: Dolphin, D., Ed. *The Porphyrins*; Academic: New York, 1978–1979; Vol. I–VII.
(3) See: Smith, K. M., *Porphyrins and Metalloporphyrins*, Elsevier: New York, 1975.
(4) Grigg R. In *The Porphyrins*; Dolphin, D., Ed.; Academic: New York, 1978; Vol. II, Chapter 10.
(5) Hush, N. S.; Dyke, J. M.; Williams, M. L.; Woolsey, I. S. *Mol. Phys.* **1969**, *17*, 559.
(6) Dyke, J. M.; Hush, N. S.; Williams, M. L.; Woolsey, I. S. *Mol. Phys.* **1971**, *20*, 1149.
(7) Hush, N. S.; Dyke, J. M.; Williams, M. L.; Woolsey, I. S. *J. Chem. Soc., Dalton Trans.* **1974**, 395.
(8) Matsuda, Y.; Yamada, S.; Murakami, Y. *Inorg. Chim. Acta* **1980**, *44*, L309.
(9) Boschi, T.; Licoccia, S.; Paolesse, R.; Tagliatesta, P.; Tehran, M. A.; Pelizzi, G.; Vitali, F. *J. Chem. Soc., Dalton Trans.* **1990**, 463.
(10) Hitchcock, P. B.; McLaughlin, G. M. *J. Chem. Soc., Dalton Trans.* **1976**, 1927.

0020-1669/92/1331-2305$03.00/0

of corrins (1.90 Å),[11] but shorter than those reported for cobalt(III) porphyrins which vary between 1.95 and 1.98 Å depending upon the axial ligand.[12] Metallocorroles also differ from metalloporphyrins in that the stable form of the central metal is generally in a higher oxidation state than that of the corresponding metalloporphyrin due to the −3 charge of the corrole macrocycle.

Early characterizations of metallocorroles concentrated on methods for synthesizing different complexes and on ligand binding equilibria of mainly cobalt derivatives which were compared to the related vitamin B_{12} coenzyme.[13-28] More recently, a number of stable new corrole complexes containing other transition[29,30] and main[31] group central metals have been synthesized and characterized, in large part, by UV–visible and NMR spectroscopy.

Very little is known about the electrochemistry of metallocorroles. A brief report on the cyclic voltammetry of chromium(V)[24] and molybdenum(V)[25] oxo corroles appeared in 1981 and some classical polarographic and voltammetric data were reported for the reduction of nickel(II) and cobalt(II) derivatives almost 20 years ago.[18,19] The Co(III)/Co(II) reaction of different corroles was investigated under several solvent conditions as was the first oxidation of the Co(III) complexes to give corrole π cation radicals. However, no mechanistic details were presented, nor were any additional oxidations or reductions reported. As will be shown in this paper, a total of two reductions and three oxidations may be observed for cobalt corroles under certain solution conditions. These are characterized in the present manuscript which also presents the first detailed electrochemistry of a rhodium(III) corrole. The investigated compounds are represented as (OMC)Rh(PPh_3) and (OMC)Co(PPh_3) where OMC is the trianion of 2,3,7,8,12,13,17,18-octamethylcorrole. These two compounds, whose structures are shown below, were electrochemically characterized in four different nonaqueous solvents and allow for the first detailed comparison of corrole redox properties with those of the very well-studied metalloporphyrins.

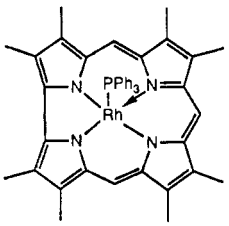

(OMC)Rh(PPh_3)

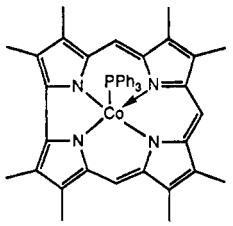

(OMC)Co(PPh_3)

(11) Venkatesan, K.; Dale, D.; Hodgkin, D. C.; Nockolds, C. E.; Moore, F. H.; O'Connor, B. H. *Proc. R. Soc. London* **1971**, A323, 455.
(12) Scheidt, W. R.; Lee, Y. *J. Struct. Bonding* **1987**, *64*, 41–42.
(13) Johnson, A. W.; Kay, I. T. *J. Chem. Soc.* **1965**, 1620.
(14) Melent'eva, T. A.; Pekel', N. D.; Berezovskii, V. M. *Russ. Chem. Rev. (Engl. Transl.)* **1969**, *38*, 2016.
(15) Johnson, A. W. *Pure Appl. Chem.* **1970**, *23*, 375.
(16) Grigg, R.; Hamilton, R. J.; Jozefowicz, M. L.; Rochester, C. H.; Terrel, R. J.; Wickwar, H. *J. Chem. Soc., Perkin Trans. 2* **1973**, 407.
(17) Hush, N. S.; Woolsey, I. S. *J. Am. Chem. Soc.* **1972**, *94*, 4107.
(18) Hush, N. S.; Dyke J. M. *J. Inorg. Nucl. Chem.* **1973**, *35*, 4341.
(19) Conlon, M.; Johnson, A. W.; Overend, W. R.; Rajapaksa, D.; Elson, C. M. *J. Chem. Soc., Perkin Trans. 1* **1973**, 2281.
(20) Hush, N. S.; Woolsey, I. S. *J. Chem. Soc., Dalton Trans.* **1974**, 24.
(21) Murakami, Y.; Matsuda, Y.; Yamada, S. *Chem. Lett.* **1977**, 689.
(22) Murakami, Y.; Yamada, S.; Matsuda, Y.; Sakada, K. *Bull. Chem. Soc. Jpn.* **1978**, *51*, 123.
(23) Murakami, Y.; Aoyama, Y.; Hayashida, M. *J. Chem. Soc., Chem. Commun.* **1980**, 501.
(24) Murakami, Y.; Matsuda, Y.; Yamada, S. *J. Chem. Soc. Dalton Trans.* **1981**, 855.
(25) Matsuda, Y.; Yamada, S.; Murakami, Y. *Inorg. Chem.* **1981**, *20*, 2239.
(26) Murakami, Y.; Aoyama, Y.; Tada, T. *Inorg. Chim. Acta* **1981**, *54*, L111.
(27) Marakami, Y.; Matsuda, Y.; Sakata, K.; Yamada, S.; Tanaka, Y.; Aoyama, Y. *Bull. Chem. Soc. Jpn.* **1981**, *54*, 163.
(28) Melent'eva, T. A. *Russ. Chem. Rev. (Engl. Transl.)* **1983**, *52*, 641.
(29) Boschi, T.; Licoccia, S.; Paolesse, R.; Tagliatesta, P. *Inorg. Chim. Acta* **1988**, *141*, 169.
(30) Licoccia, S.; Paci, M.; Paolesse, R.; Boschi, T. *J. Chem. Soc., Dalton Trans.* **1991**, 461.
(31) Paolesse, R.; Licoccia, S.; Boschi, T. *Inorg. Chim. Acta* **1990**, *178*, 9.

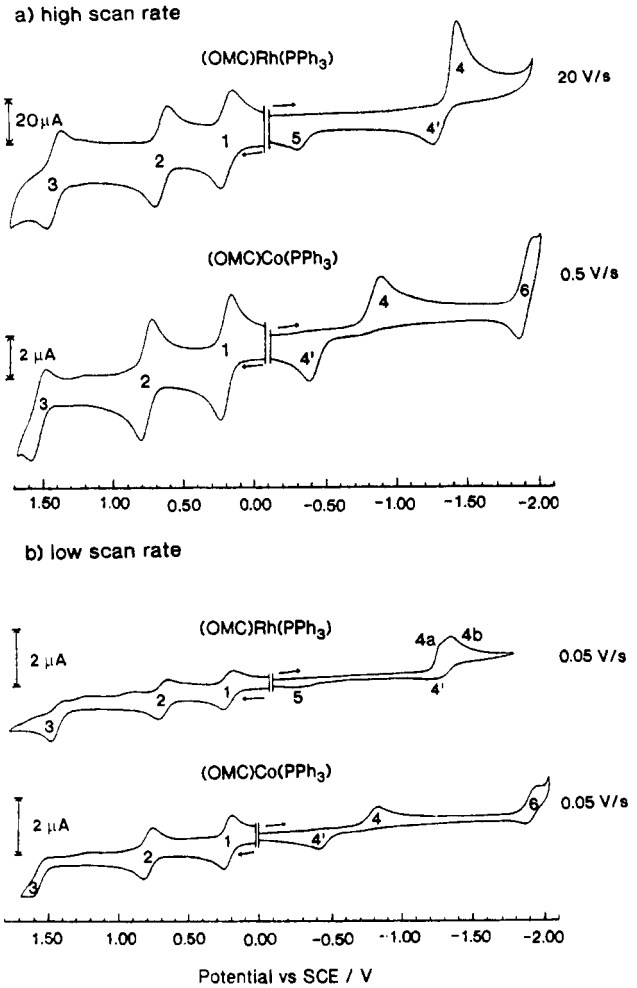

Figure 1. Cyclic voltammograms of 1.32 mM (OMC)Rh(PPh_3) and 1.65 mM (OMC)Co(PPh_3) in PhCN containing 0.10 M TBAP at (a) high potential scan rate and (b) low potential scan rate.

Experimental Section

Chemicals. Reagent grade benzonitrile (PhCN), from Aldrich Chemical Co., was vacuum-distilled over P_2O_5. HPLC grade *N,N*-dimethylformamide (DMF), from Aldrich Chemical Co., was used as received. Spectroscopic grade dichloromethane (CH_2Cl_2), from J. T. Baker, Inc., or Mallinckrodt, Inc., was washed with sulfuric acid until the disappearance of a yellowish color in the acid layer, after which it was twice washed with water and distilled first over P_2O_5 and then over CaH_2. Tetrahydrofuran (THF), from Mallinckrodt, Inc., was distilled over $LiAlH_4$. Triphenylphosphine (PPh_3), from Aldrich Chemical Co., was recrystallized from ethanol and dried in a vacuum oven at 40 °C prior to use. Tetrabutylammonium perchlorate (TBAP), from Eastman Kodak Co., was twice recrystallized from absolute ethanol and stored under vacuum at 40 °C.

(2,3,7,8,12,13,17,18-Octamethylcorrolato)(triphenylphosphine)cobalt(III), (OMC)Co(PPh_3),[19] and carbonyl(2,3,7,8,12,13,17,18-octamethylcorrolato)(triphenylphosphine)rhodium(III), (OMC)Rh(PPh_3)(CO),[29] were prepared as described in the literature. Carbon monoxide is easily dissociated from (OMC)Rh(PPh_3)(CO) in solution (as ascertained by the disappearance of the ν_{CO} band), and this leads to the formation of (OMC)Rh(PPh_3), which was characterized in the present study under an N_2 atmosphere. The chemical reduction of (OMC)Co(PPh_3) in DMF was carried out using excess $NaBH_4$ from Aldrich, and the UV–visible spectrum of the product was measured directly in a 1-cm cuvette without prior separation.

Instrumentation. Cyclic voltammograms were obtained with a three-electrode system using one of four different experimental setups. These were an EG&G Princeton Applied Research Model 174A/175 polarographic analyzer/universal programmer, an EG&G PAR Model 173/175 potentiostat/universal programmer, an IBM EC 225 voltammetric analyzer, and a BAS 100 electrochemical analyzer. Spectroelectrochemistry was performed with a Tracor Northern Model 6500 multichannel spectrometer. Electronic absorption spectra of the neutral compounds were also recorded with a double-beam IBM 9430 spectropho-

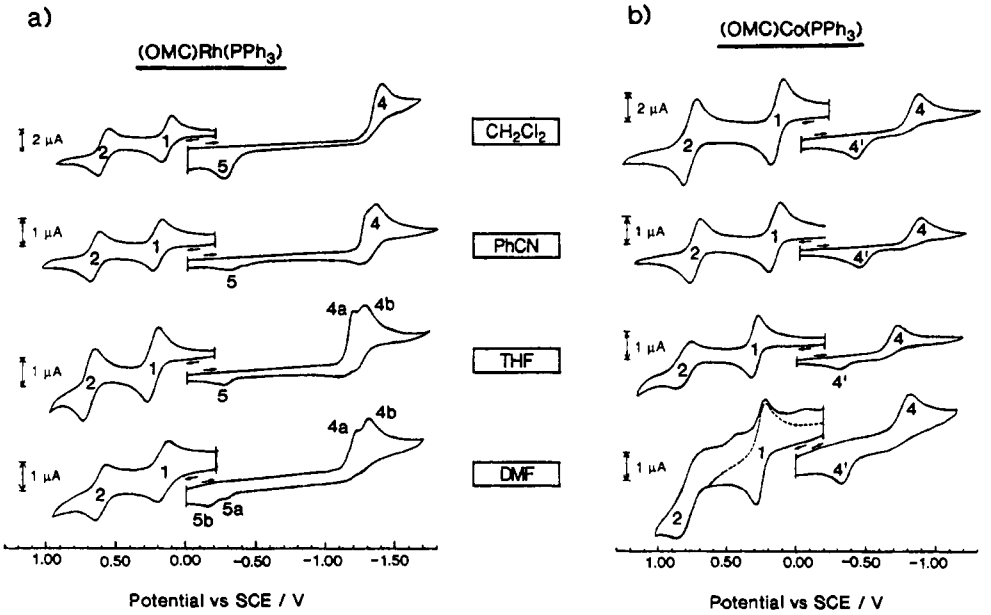

Figure 2. Room-temperature cyclic voltammograms of (a) (OMC)Rh(PPh_3) and (b) (OMC)Co(PPh_3) in four nonaqueous solvents at a scan rate of 0.1 V/s.

tometer. The three-electrode system consisted of a Pt disk working electrode, a saturated calomel reference electrode (SCE) and a Pt-wire counter electrode. The thin-layer spectroelectrochemical cell has been previously described.[32]

Results

Electrochemistry of (OMC)Rh(PPh_3) and (OMC)Co(PPh_3). Both corrole complexes undergo up to three one-electron oxidations depending upon solvent. The number of abstracted electrons was calculated by controlled-potential coulometry as well as by analysis of the current–voltage curves obtained by cyclic voltammetry. All three oxidations are reversible in PhCN at high scan rates, and this is shown by the two cyclic voltammograms in Figure 1a. The oxidations are labelled as processes 1–3 and, for the case of (OMC)Rh(PPh_3), are located at $E_{1/2}$ = 0.21, 0.66, and 1.42 V. The first oxidation of (OMC)Co(PPh_3) occurs at a similar potential of 0.19 V in PhCN while the latter two processes are shifted positively in potential and occur at $E_{1/2}$ = 0.76 and 1.54 V. The first two one-electron abstractions of both compounds are reversible at all scan rates but the third oxidation becomes irrversible at lower potential sweep rates as illustrated in Figure 1b. The values of $|E_{pa} - E_{pc}|$ for the first two oxidations vary between 60 and 70 mV and the peak current increases linearly with $v^{1/2}$ over a range of potential sweep rates, v, between 0.02 and 5 V/s. These data clearly indicate diffusion-controlled one-electron transfer processes.

The (OMC)Rh(PPh_3) complex is irreversibly reduced in a single multielectron-transfer step and the cathodic peak potential is located at E_p = −1.45 V for a scan rate of 20 V/s. This reaction is labeled as process 4 in Figure 1a. Two reoxidation peaks are associated with the reduction and these are located at E_p = −1.26 (peak 4′) and −0.32 V (peak 5) at a scan rate of 20 V/s. The peak current for reduction of (OMC)Rh(PPh_3) (process 4) is double the peak current for the first oxidation of the same complex (process 1) at a scan rate of 20 V/s, and it is also approximately double the peak current for the anodic process at E_p = −1.26 V (peak 4′). The reduction of (OMC)Rh(PPh_3) is irreversible at all scan rates, but this process is split into two overlapping peaks at lower scan rates as shown in Figure 1b. Under these conditions the reductions are labeled as 4a and 4b.

(OMC)Co(PPh_3) undergoes two one-electron reductions in all of the investigated solvents. The first (peak 4) is irreversible and occurs at E_p = −0.90 V in PhCN at a scan rate of 0.5 V/s. This reduction is coupled to a reoxidation peak at E_p = −0.36 V (peak 4′). The second reduction of (OMC)Co(PPh_3) (process 6) occurs at $E_{1/2}$ = −1.92 V in PhCN and is reversible at all scan rates. A similar room-temperature electrochemistry is observed for (OMC)Co(PPh_3) in CH_2Cl_2, THF and DMF. Examples of the resulting cyclic voltammograms for (OMC)Co(PPh_3) and (OMC)Rh(PPh_3) in all four solvents are shown in Figure 2, and a summary of half-wave potentials for oxidation and reduction of the two complexes in each solvent is given in Table I.

Table I. Half-Wave Potentials (V vs SCE) for (OMC)Rh(PPh_3) and (OMC)Co(PPh_3)[a]

metal system	solvent	DN[b]	oxidation 1st	oxidation 2nd	oxidation 3rd	reduction[c] 1st	reduction[c] 2nd
Rh(III)	CH_2Cl_2	0.0	0.15	0.61	1.43[d]	−1.39	−1.39
	PhCN	11.9	0.21	0.66	1.42	−1.27	−1.34
	THF	20.0	0.23	0.67		−1.20	−1.29
	DMF	26.6	0.16	0.61		−1.21	−1.31
Co(III)	CH_2Cl_2	0.0	0.18	0.80	~1.68[d,e]	−0.85	−1.90
	PhCN	11.9	0.19	0.76	1.54	−0.86	−1.92[f]
	THF	20.0	0.30	~0.80[e]		−0.72	−1.84[f,g]
	DMF	26.6	0.25	0.83[d]		−0.79	−1.83[g]

[a] All solvents contained 0.1 M TBAP except for THF which contained 0.20 M TBAP as supporting electrolyte. [b] Gutmann solvent donor number.[38] [c] Unless otherwise indicated, all values are given as E_p for a scan rate of 0.1 V/s. [d] E_p at a scan rate of 0.1 V/s. [e] Uncertainty in the value due to presence of two overlapping peaks. [f] Reversible $E_{1/2}$. [g] Value obtained at −70 °C.

The electrochemistry of (OMC)Rh(PPh_3) and (OMC)Co(PPh_3) was investigated at room and low temperatures, and examples of the resulting cyclic voltammograms at 23 and −70 °C in THF are given in Figure 3. The reduction of (OMC)Rh(PPh_3) is split into two processes at room temperature for a scan rate of 0.1 V/s but these two processes are overlapped at −70 °C in THF (see Figure 3a). This leads to a cyclic voltammogram which is similar to the one obtained in PhCN at room temperature for a scan rate of 20 V/s (Figure 1a). In addition, the peak current for process 5 at E_p = −0.28 V is decreased in intensity while that for process 4′ is increased.

No temperature dependent changes are observed for oxidation of (OMC)Rh(PPh_3) (see Figure 3a) but this is not the case for (OMC)Co(PPh_3) (Figure 3b) where the second oxidation (peak 2) is split into two separate processes. The heights of the two peaks are approximately equal at −70 °C and each is about half of the current for peaks 1 and 3. This suggests an equilibrium between two separate forms of the doubly oxidized corrole. A similar

(32) Lin, X. Q.; Kadish, K. M. *Anal. Chem.* **1985**, *57*, 1498.

Table II. Electronic Absorption Data of Neutral and Electrogenerated (OMC)Co(PPh_3) and (OMC)Rh(PPh_3)

metal system	electrode reacn	solvent	reacn product[a]	λ_{max}, nm ($\epsilon \times 10^{-4}/M^{-1}$ cm^{-1})		
Co(III)	none	CH_2Cl_2	(OMC)$Co^{III}(PPh_3)$	367 (4.95)	530 (0.58)	573 (1.10)
		PhCN		367 (4.86)	532 (0.73)	573 (1.13)
		THF		367 (4.47)	533 (0.70)	573 (1.11)
		DMF		367 (4.74)	530 (0.66)	574 (1.03)
	1st redn	CH_2Cl_2	$[(OMC)Co^{II}]^-$	405 (7.8)	533 (1.3)	
		PhCN		408 (7.1)	534 (1.5)	
		DMF		407 (7.2)	533 (1.2)	
	2nd redn	DMF	$[(OMC)Co^{I}]^{2-}$	400 (9.3)		
	1st oxidn	PhCN	$[(OMC)Co^{III}(PPh_3)]^+$	351 (3.8)	642 (0.6)	
	2nd oxidn	PhCN	$[(OMC)Co^{III}(PPh_3)]^{2+}$	333 (3.9)		
Rh(III)	none	PhCN	(OMC)$Rh^{III}(PPh_3)$	417 (5.39)	555 (1.52)	
	1st oxidn	PhCN	$[(OMC)Rh^{III}(PPh_3)]^+$	420 (3.4)	652 (0.5)	
	2nd oxidn	PhCN	$[(OMC)Rh^{III}(PPh_3)]^{2+}$	402 (2.6)		
	1st oxidn	PhCN/PPh_3[b]	$[(OMC)Rh^{III}(PPh_3)_2]^+$	347	445	

[a] Identity of product proposed on the basis of spectroscopic and electrochemical data. [b] Spectrum obtained in PhCN containing 0.10 M PPh_3.

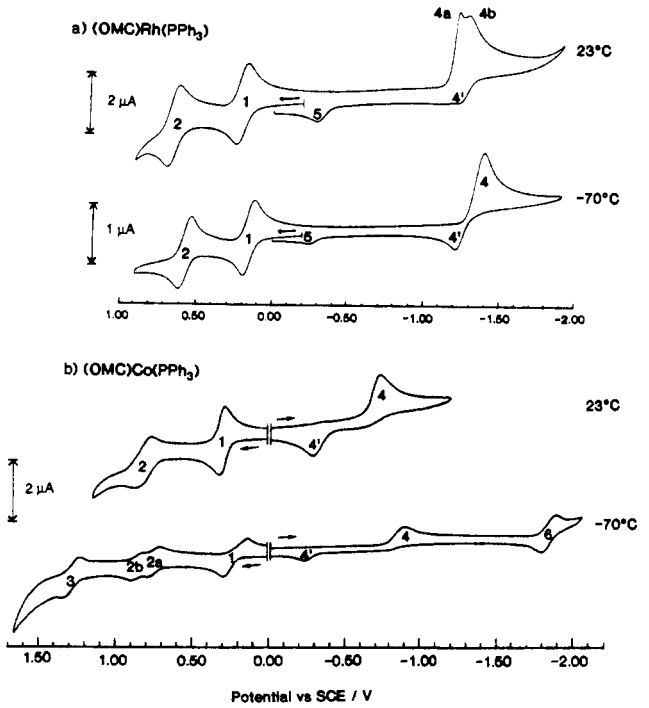

Figure 3. Room- and low-temperature cyclic voltammograms of (a) (OMC)Rh(PPh_3) (v = 0.1 V/s) and (b) (OMC)Co(PPh_3) (v = 0.2 V/s) in THF containing 0.20 M TBAP.

low-temperature cyclic voltammogram is obtained in DMF.

Spectral Characterization of Oxidized and Reduced Complexes. Thin-layer UV–visible spectra taken during the first one-electron oxidation of (OMC)Rh(PPh_3) and (OMC)Co(PPh_3) in PhCN are shown in Figure 4. The intensity of the Soret-like band decreases after abstraction of one electron from (OMC)Rh(PPh_3) or (OMC)Co(PPh_3). Isosbestic points are obtained during each reaction, indicating the lack of a spectrally detectable intermediate. The electrooxidations are reversible, and there is no evidence for a coupled chemical reaction. The final spectrum after the second one-electron oxidation of (OMC)Rh(PPh_3) is characterized by a broad ill-defined band between 350 and 450 nm while doubly oxidized (OMC)Co(PPh_3) has a single band centered at 333 nm. These reactions are also reversible by thin-layer spectroelectrochemistry and the resulting UV–visible spectra are shown in Figure 5.

Electronic absorption spectra obtained during reduction of (OMC)Co(PPh_3) at −0.90 V in DMF are shown in Figure 6a. The final spectrum after addition of one electron is identical with the spectrum obtained after a chemical reduction of (OMC)-Co(PPh_3) by excess $NaBH_4$ in DMF (see Figure 6b). This spectrum is also identical to the one obtained by controlled-potential reduction of (OMC)Co(PPh_3) at −0.90 V in PhCN. The

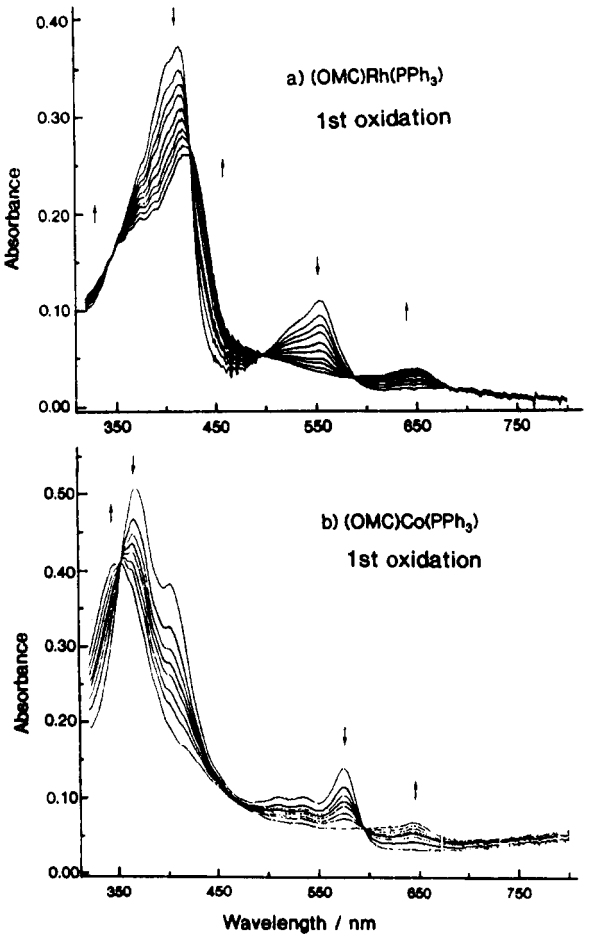

Figure 4. Time-resolved thin-layer spectra obtained during the controlled-potential one-electron oxidation of (a) (OMC)Rh(PPh_3) and (b) (OMC)Co(PPh_3) at 0.40 V in PhCN containing 0.20 M TBAP.

conversion of (OMC)Co(PPh_3) to its singly reduced form is reversible, and the initial spectrum of the starting compound could be regenerated by application of a constant controlled potential positive of peak 4′. Time-resolved thin-layer spectra were also measured during the second reduction of (OMC)Co(PPh_3) in DMF, and a summary of the resulting UV–visible spectral data, as well as those of the neutral and oxidized (OMC)Rh(PPh_3) and (OMC)Co(PPh_3) complexes, is given in Table II.

The cyclic voltammograms of (OMC)Rh(PPh_3) show two discrete reduction peaks at low potential scan rates (see Figures 1–3), and different UV–visible spectra of the reduced complexes are obtained depending upon the potential selected for the controlled-potential reduction. The spectral changes obtained in PhCN during electrolysis of (OMC)Rh(PPh_3) at −1.27 V (a potential between peaks 4a and 4b) are shown in Figure 7a while

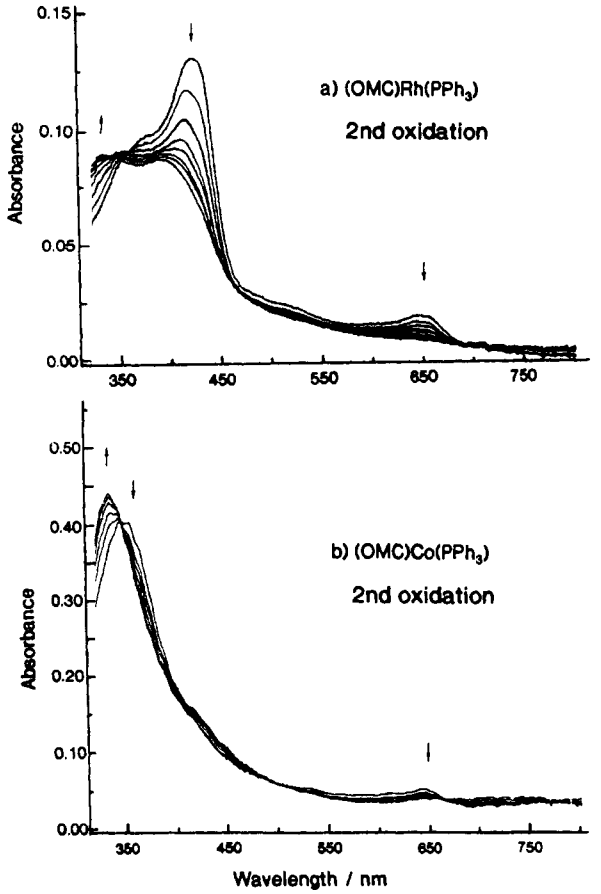

Figure 5. Time-resolved thin-layer spectra obtained during the controlled-potential one-electron oxidation of (a) $[(OMC)Rh(PPh_3)]^+$ and (b) $[(OMC)Co(PPh_3)]^+$ at 1.00 V in PhCN containing 0.20 M TBAP.

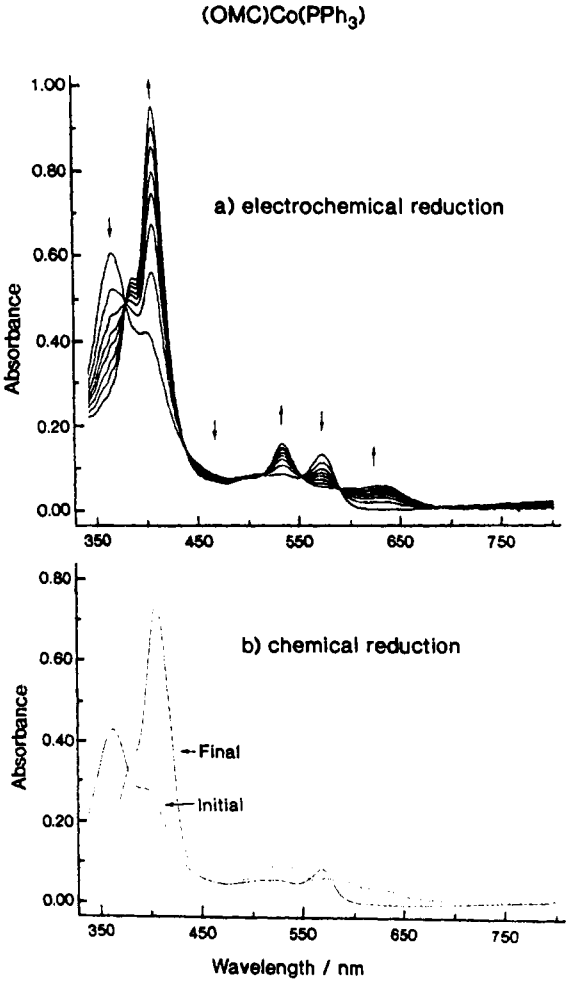

Figure 6. UV–visible spectra of neutral and singly-reduced (OMC)Co(PPh_3) (a) by controlled-potential electrolysis at −0.90 V in DMF, 0.20 M TBAP and (b) by reaction with excess $NaBH_4$ in DMF.

those obtained at −1.60 V are shown in Figure 7b. Neither of the two reductions is reversible, as indicated by the fact that the UV–visible spectra obtained after reoxidation at −0.10 V do not coincide with the original spectrum of the starting species.

Electrochemistry of (OMC)Rh(PPh_3) and (OMC)Co(PPh_3) in PhCN/PPh_3 Mixtures. The electrochemistry of (OMC)Rh(PPh_3) and (OMC)Co(PPh_3) was investigated in the presence of PPh_3 to determine the fate of the bound PPh_3 axial ligand after electrooxidation or electroreduction of each complex. Both the first oxidation (peak 1) and the two reductions (peaks 4 and 6) of (OMC)Co(PPh_3) are unaffected by PPh_3 addition to solution and the resulting cyclic voltammograms in PhCN containing between 0 and 100 equiv of PPh_3 are shown in Figure 8. The second oxidation becomes irreversible after the addition of 1.0 equiv of PPh_3 to solution, and no further changes are observed up to the addition of 500 equiv of PPh_3, the highest concentration investigated. The third oxidation of the cobalt or rhodium corroles could not be investigated in the PhCN/PPh_3 mixtures due to an oxidation of PPh_3, which occurs at a more negative potential.

Several changes are observed in the cyclic voltammograms of (OMC)Rh(PPh_3) in PhCN as PPh_3 is added to solution. The first oxidation (process 1) shifts negatively in potential while the second becomes irreversible. The addition of PPh_3 also results in an increased anodic peak current for process 4 and this is shown in Figures 9 and 10. A plot of $E_{1/2}$ for the first oxidation of (OMC)Rh(PPh_3) vs log $[PPh_3]$ gives a straight line with a slope of −0.056 V (see Figure 10), and this value may be compared to a theoretically expected slope of −0.059 V for the electrode reaction given in eq 1.

$$[(OMC)Rh^{III}(PPh_3)_2]^+ + e^- \rightleftarrows (OMC)Rh^{III}(PPh_3) + PPh_3 \quad (1)$$

The formation constant of the bis(phosphine) complex was calculated using the data in Figure 10 and the measured $E_{1/2}$ = 0.21 V for oxidation of (OMC)Rh(PPh_3) in PhCN containing 0.10 M TBAP. The value of K, obtained by extrapolation of the plot to $[PPh_3]$ = 1 M, is 8×10^2, and this formation constant corresponds to the reaction given in eq 2.

$$[(OMC)Rh^{III}(PPh_3)]^+ + PPh_3 \rightleftarrows [(OMC)Rh^{III}(PPh_3)_2]^+ \quad (2)$$

The anodic peak current for process 4 increases with increase in PPh_3 concentration and this is quantitatively shown in Figure 10b by the plot of i_{pa}/i_{pc} at a scan rate of 0.1 V/s. The ratio of anodic to cathodic peak current for process 4 also depends upon scan rate as illustrated in Figures 11 and 12. The ratio of i_{pa}/i_{pc} = 0.23 at 0.02 V/s and 0.90 at 20 V/s in the presence of 500 equiv of PPh_3. The transformation between the two extremes is graphically shown in Figure 12. The maximum peak current for process 4 is double that of process 1 at a scan rate of 20 V/s but increases by about 20% at lower scan rates as shown in Figure 12b.

The spectral changes obtained during the first oxidation of (OMC)Rh(PPh_3) in PhCN containing 0.10 M PPh_3 and 0.10 M TBAP are different from those in PhCN containing 0.10 M TBAP. This behavior is consistent with the voltammetric data, which indicate formation of $[(OMC)Rh(PPh_3)_2]^+$ in PhCN/PPh_3 mixtures. The spectrum of this bis(phosphine) adduct is shown in Figure 13 and is characterized by two well-defined bands at 347 and 445 nm. There is no effect of PPh_3 on the spectra of the electroreduced (OMC)Rh(PPh_3) complexes. The UV–visible spectrum after electrolysis at −1.60 V in PhCN containing PPh_3 and TBAP is similar to the one obtained after reduction of the same compound in PhCN containing TBAP (see Figure 7b).

Discussion

Oxidation of (OMC)Rh(PPh_3) and (OMC)Co(PPh_3). The electrooxidation of the two complexes is straightforward and can

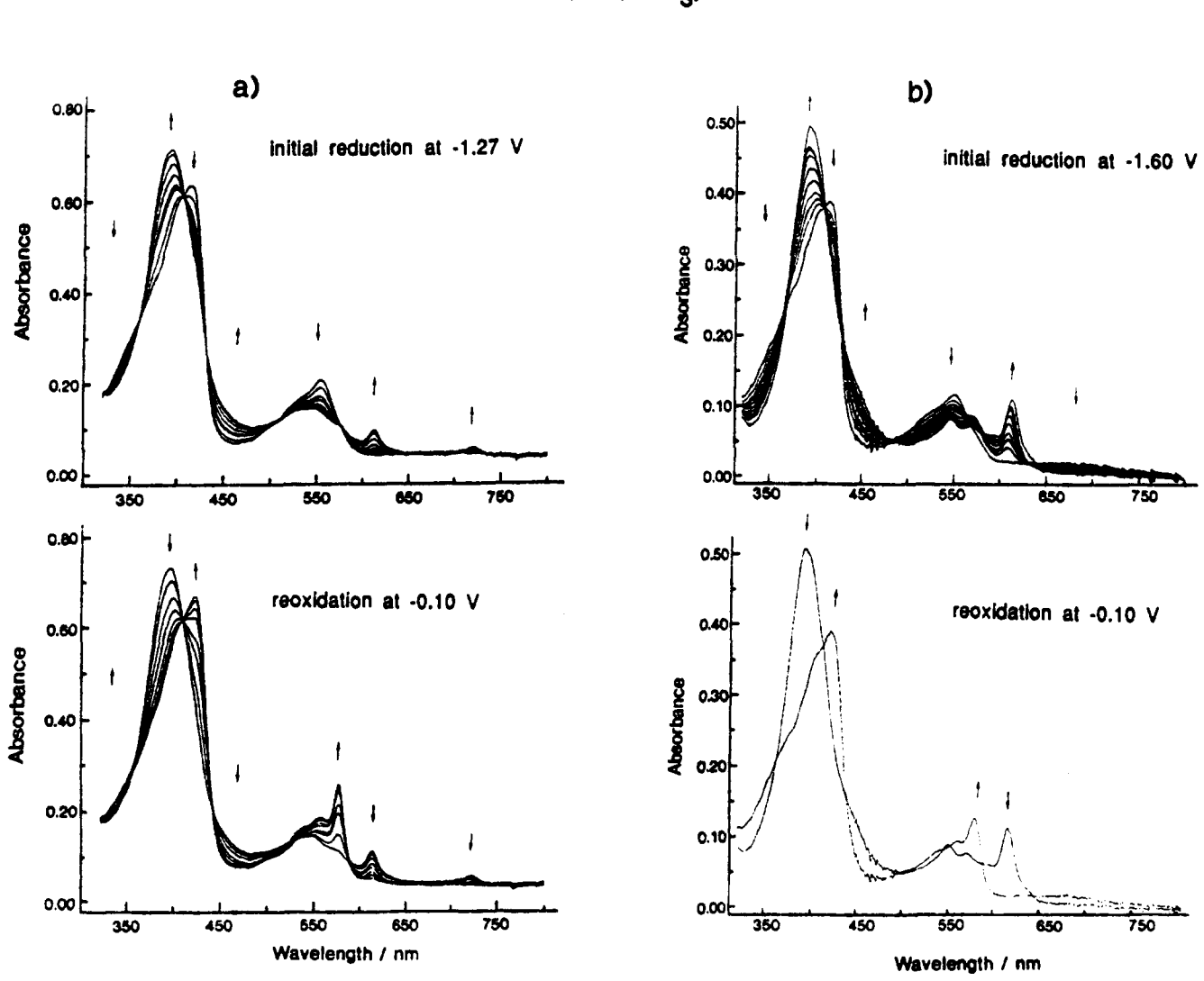

Figure 7. Thin-layer UV–visible spectral changes of (OMC)Rh(PPh_3) in PhCN containing 0.10 M TBAP (a) during controlled potential reduction at −1.27 V followed by reoxidation at −0.10 V and (b) during controlled potential reduction at −1.60 V followed by reoxidation at −0.10 V.

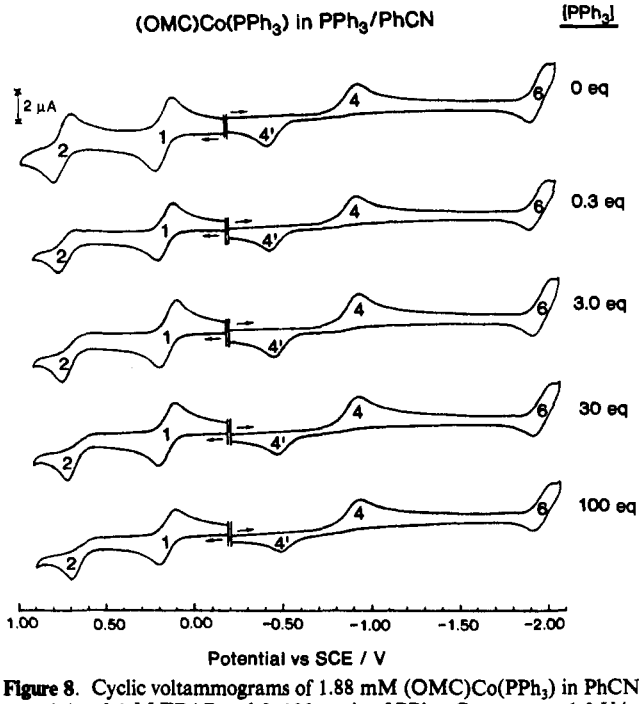

Figure 8. Cyclic voltammograms of 1.88 mM (OMC)Co(PPh_3) in PhCN containing 0.1 M TBAP and 0–100 equiv of PPh_3. Scan rate = 1.0 V/s.

be accounted for by the reactions given in eqs 3–5, where M = Co or Rh.

$$(OMC)M^{III}(PPh_3) \rightleftarrows [(OMC)M^{III}(PPh_3)]^+ + e^- \quad (3)$$

$$[(OMC)M^{III}(PPh_3)]^+ \rightleftarrows [(OMC)M^{III}(PPh_3)]^{2+} + e^- \quad (4)$$

$$[(OMC)M^{III}(PPh_3)]^{2+} \rightleftarrows [(OMC)M^{III}(PPh_3)]^{3+} + e^- \quad (5)$$

The three oxidation potentials are similar for both compounds in PhCN (see Figure 1 and Table I). The formation of Co(IV) and Rh(IV) derivatives are unlikely, and the electrochemical reactions should involve a stepwise formation of mono-, di-, and trications in which all of the electrons are abstracted from the corrole π ring system. The third oxidation of both complexes is irreversible in CH_2Cl_2, and this reaction is not observed in THF or DMF, both of which have a decreased positive potential limit compared to CH_2Cl_2 or PhCN. There is no evidence for a metal-centered oxidation of (OMC)Rh(PPh_3) or (OMC)Co(PPh_3) and this is also the case for cobalt(III) and rhodium(III) porphyrins, all of which are oxidized at the porphyrin π ring system.[1]

As graphically shown in Figure 14, the first oxidation of (OMC)M(PPh_3) occurs at potentials which are 780–810 mV more negative than for oxidation of a metalloporphyrin such as $(TPP)Rh^{III}(CH_3)$ or $(TPP)Co^{III}(CH_3)$ where TPP is the dianion of *meso*-tetraphenylporphyrin.[33] The more facile oxidation of

(33) Kadish, K. M.; Han, B. C.; Endo, A. *Inorg. Chem.* **1991**, *30*, 4502.

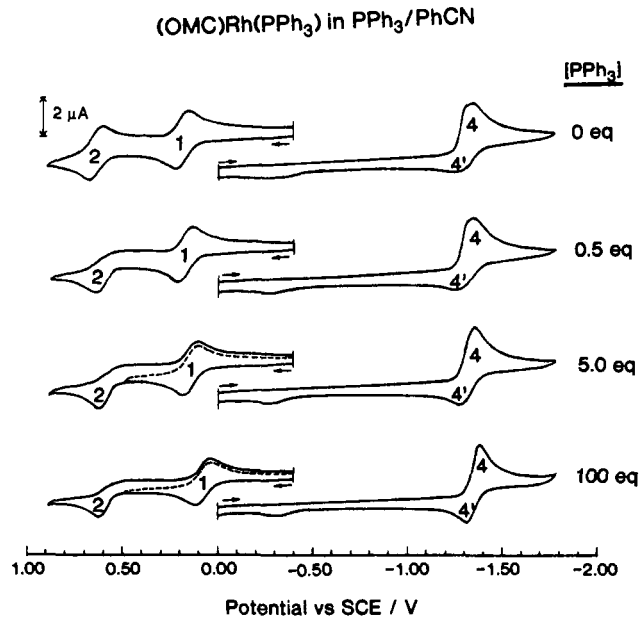

Figure 9. Cyclic voltammograms of 1.15 mM (OMC)Rh(PPh_3) in PhCN containing 0.1 M TBAP and 0–100 equiv of PPh_3. Scan rate = 0.10 V/s.

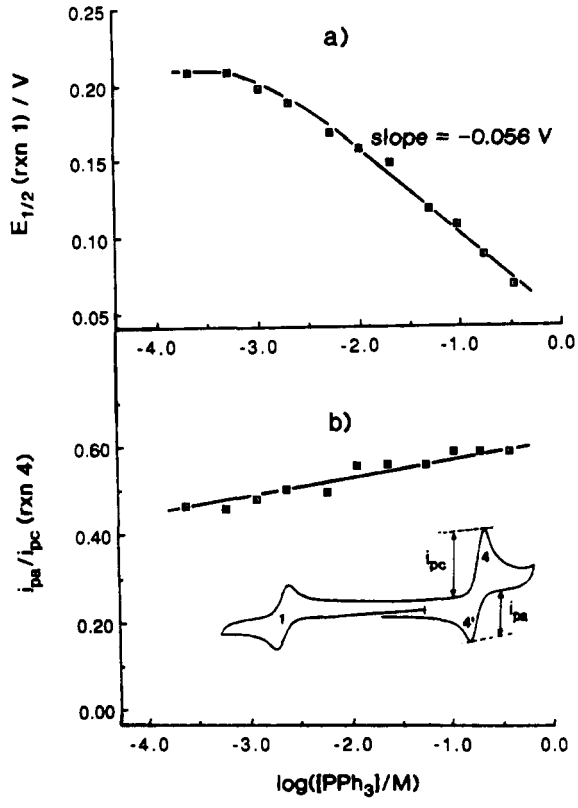

Figure 10. PPh_3 concentration dependence of (a) $E_{1/2}$ for reaction 1 of (OMC)Rh(PPh_3) at a scan rate of 0.1 V/s and (b) the i_{pa}/i_{pc} ratio for reaction 4 under the same solution conditions. Data were taken from cyclic voltammograms of the type shown in Figure 9.

the rhodium(III) corrole with respect to the analogous rhodium(III) porphyrins is in agreement with previously reported XPS data[34] which shows that the Rh 3d binding energy of (OMC)Rh(PPh_3) is lower than that of porphyrins; i.e., the rhodium atom is more negative, in agreement with the trianionic structure of the corrole moiety. This results in a more basic macrocyclic ring due to a simple inductive effect, and the net result is an easier

(34) Zanoni, R.; Boschi, T.; Licoccia, S.; Paolesse, R.; Tagliatesta, P. *Inorg. Chim. Acta* **1988**, *145*, 175.

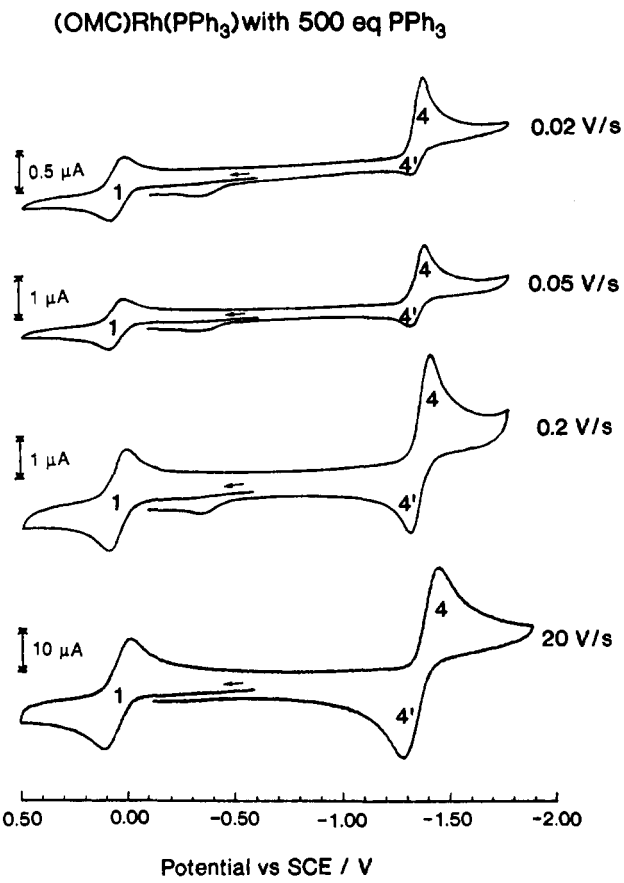

Figure 11. Scan rate dependence of cyclic voltammograms for the first reduction and first oxidation of 1.15 mM (OMC)Rh(PPh_3) in PhCN containing 0.10 M TBAP and 0.575 M PPh_3.

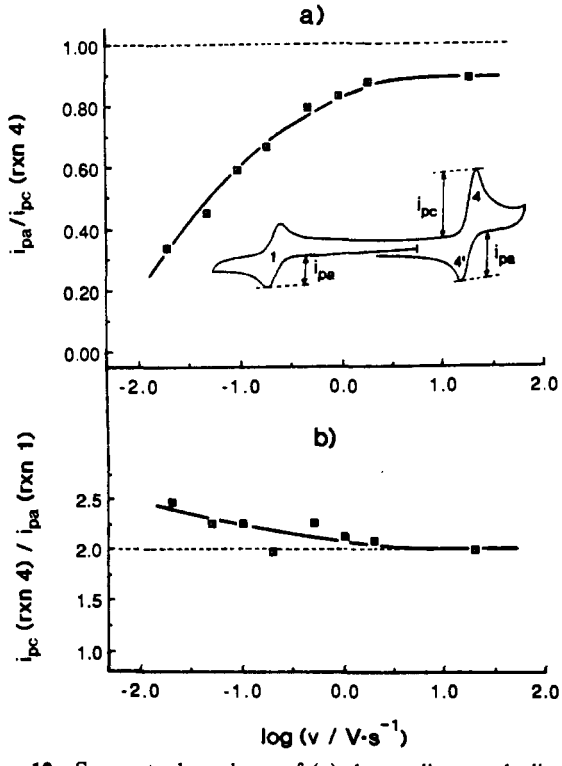

Figure 12. Scan rate dependence of (a) the anodic to cathodic peak current ratio for reaction 4 of 1.15 mM (OMC)Rh(PPh_3) in PhCN containing 0.1 M TBAP and 0.575 M PPh_3 and (b) i_{pc} (reaction 4)/i_{pc} (reaction 1) ratio under the same solution conditions.

oxidation of (OMC)M^{III}(PPh_3).

The absolute potential difference between the first two oxidations of (OMC)Rh(PPh_3) amounts to 450 mV in PhCN and

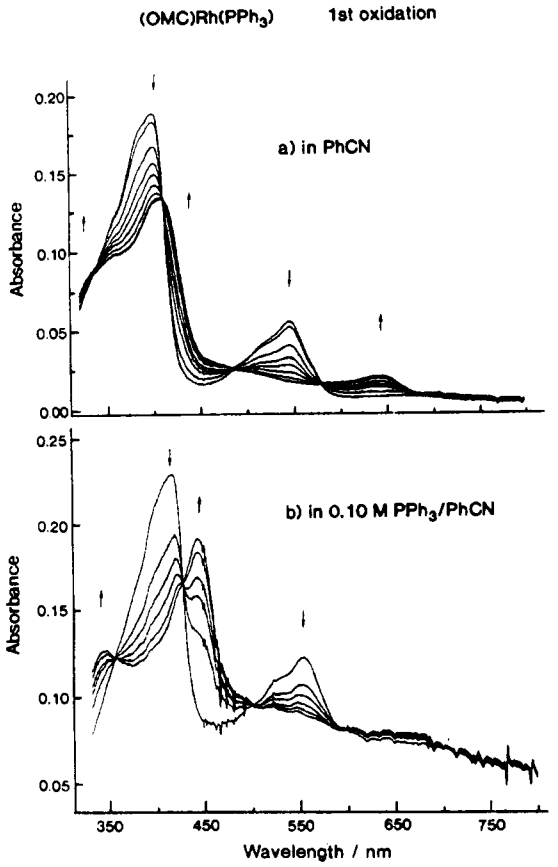

Figure 13. UV–visible spectral changes during the controlled-potential one-electron oxidation of (OMC)Rh(PPh_3) at +0.40 V in (a) PhCN containing 0.20 M TBAP and (b) PhCN containing 0.2 M TBAP and 0.1 M PPh_3.

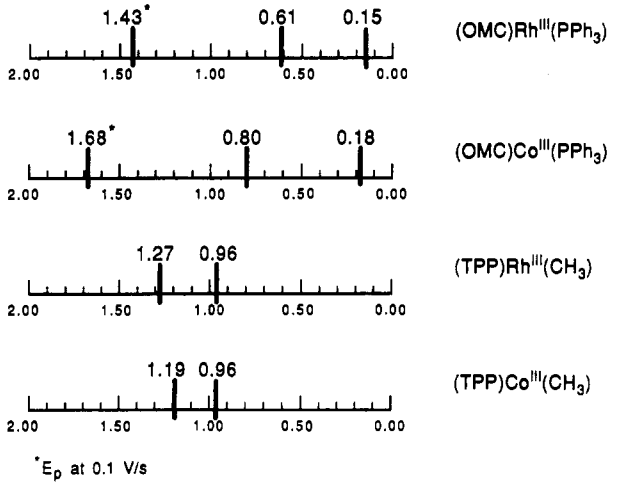

Figure 14. Half-wave potentials for the oxidations of (OMC)Rh(PPh_3), (OMC)Co(PPh_3), (TPP)Rh(CH_3), and (TPP)Co(CH_3) in CH_2Cl_2, containing 0.10 M TBAP. Data on the TPP complexes were taken from ref 33.

460 mV in CH_2Cl_2 while larger values of 570 and 620 mV are obtained for (OMC)Co(PPh_3) in the same two solvents. The absolute potential separation between the second and third oxidation of (OMC)Rh(PPh_3) is 760 mV in PhCN and 820 mV in CH_2Cl_2, and similar separations of 780 and 880 mV are observed between the second and third oxidations of (OMC)Co(PPh_3) in the same two solvents. The first separation is much greater than that for metalloporphyrins where absolute potential differences between formation of a π cation radical and dication generally range between 250 and 350 mV.[1]

Reduction of (OMC)Co(PPh_3). Two distinctly different redox couples are involved in the reduction and reoxidation of

Scheme I

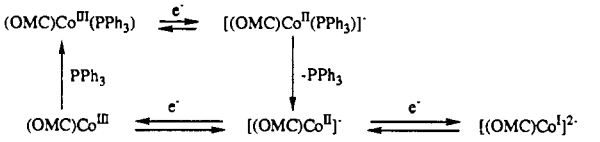

(OMC)Co(PPh_3). These are labeled as processes 4 and 4′ in Figures 1–3 and involve reversible one-electron-transfer processes followed by an irreversible chemical reaction. The values of $|E_p - E_{p/2}|$ for reactions 4 and 4′ vary between 60 and 70 mV in THF at potential scan rates of 0.02 to 0.5 V/s and a plot of E_p vs log v gives a slope of 30 mV over the same potential sweep range. This slope is consistent with an electrochemical EC type mechanism in which the electrochemical reaction (the E step) involves a reversible addition of one electron.[35]

The UV–visible spectrum of the (OMC)Co(PPh_3) is independent of solvent in CH_2Cl_2, PhCN, THF, or DMF, and this is also the case for the singly reduced product under the same experimental conditions (see Table II). The irreversible reduction of (OMC)Co(PPh_3) parallels electrochemical data in the literature for reduction of cobalt porphyrins of the type (P)CoX or $[(P)Co(S)_2]^+$ where X is a halide ion and S a solvent molecule.[1] It is proposed that the cobalt porphyrins and corroles are reduced by a similar mechanism and that the stepwise one-electron reduction of (OMC)Co(PPh_3) occurs according to the sequence of steps given in Scheme I.

The fact that (OMC)Co(PPh_3) has an electronic absorption spectrum which is independent of solvent suggests a lack of solvent binding to the initial Co(III) species and is consistent with the presence of a 5-coordinate complex where the metal ion is out of the macrocycle plane.[36] The irreversible reduction can best be ascribed to a variation of geometry which would occur upon dissociation of the PPh_3 axial ligand and formation of a square-planar Co(II) complex upon electroreduction. The generation of a cobalt(II) corrole is well documented in the literature[20] and the EPR spectrum demonstrates a 4-coordinate species with D_{4h} symmetry.

The UV–visible spectrum of singly reduced (OMC)Co(PPh_3) is characterized by bands at 408 and 534 nm in PhCN, and the species in solution is assigned as $(OMC)Co^{II}$. A similar UV–visible spectrum is obtained in CH_2Cl_2, DMF, and CH_2Cl_2 containing 1.0 M pyridine.[37] This result clearly indicates a lack of ligand binding to the Co(II) central metal of (OMC)Co. It is also consistent with the fact that the reduction peaks of (OMC)Co(PPh_3) do not vary upon addition of excess PPh_3 to solution (see Figure 8). The binding of one or more donor molecules along the z axis is known for neutral cobalt(II) porphyrins, but this reaction does not occur in the corroles, most likely because of the added negative charge on the complex. Finally, it should be noted that the same UV–visible spectrum is obtained after a chemical reduction of (OMC)Co(PPh_3) by $NaBH_4$ in DMF. This spectrum is shown in Figure 6b.

A further one-electron reduction of $[(OMC)Co^{II}]^-$ to generate $[(OMC)Co^{I}]^{2-}$ is observed at more negative potentials in all four investigated solvents (see Table I), and the resulting UV–visible spectral data of the Co(I) product in DMF are summarized in Table II. This reaction was not investigated in detail due to its proximity to the solvent discharge.

Reduction of (OMC)Rh(PPh_3). The cyclic voltammograms of (OMC)Rh(PPh_3) are characterized by either one or two closely spaced reduction peaks depending upon the specific experimental conditions. A single overlapping multielectron transfer is observed in CH_2Cl_2 but two closely spaced processes are seen in PhCN,

(35) Nicholson, R. S.; Shain I. *Anal. Chem.* **1964**, *36*, 706.
(36) The UV–visible spectrum of (OMC)Co(PPh_3) in pyridine has been assigned as the six-coordinate bis(pyridine) complex.[19] Studies in our laboratory confirm that the spectra in neat pyridine or in CH_2Cl_2 containing 1.0 M pyridine are characterized by bands at 422, 533, and 574 nm, and these differ from those obtained in the other investigated solvents (see Table II).[37]
(37) Koh, W.; Kadish, K. M. Unpublished results.

Scheme II

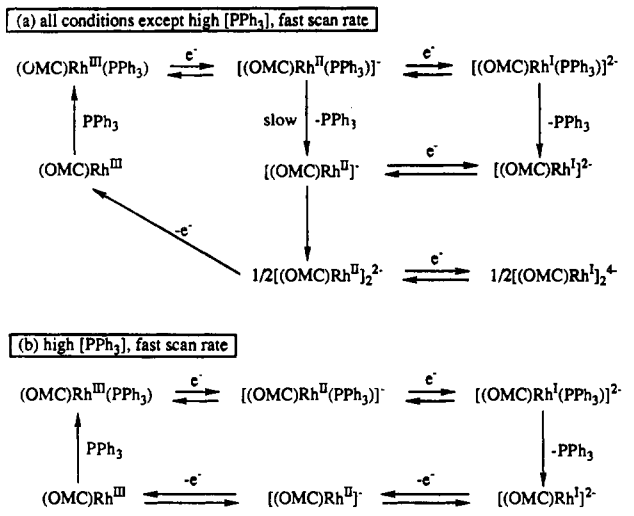

THF, or DMF (see Figure 2). The absolute potential separation between the two reduction peaks is 70 mV in PhCN, 90 mV in THF, and 100 mV in DMF (see Table I). These differences in potential parallel the Gutmann solvent donor number[38] and are consistent with a solvent stabilization of the first electroreduction product. The 180 mV potential shift in E_p upon going from CH_2Cl_2 to DMF can be interpreted in terms of a metal-centered reduction.

The values of $|E_p - E_{p/2}|$ for process 4a in Figure 1b vary between 30 and 40 mV in PhCN at potential sweep rates of 0.02–0.2 V/s, and a plot of E_p vs log v gives a slope of 35 ± 5 mV over the same potential sweep range. This suggests an electrochemical EC mechanism similar to the one shown in Scheme I for the case of (OMC)Co(PPh_3). The chemical reaction following electron addition to (OMC)Rh(PPh_3) can be slowed down by addition of excess PPh_3 to solution, and a reversible cyclic voltammogram is then obtained at fast potential scan rates as shown in Figure 11. Under these conditions, the reduction involves an overall two-electron-transfer process and the anodic peak 5 is no longer observed. This latter peak is assigned to the oxidation of $[(OMC)Rh^{II}]_2^{2-}$, and the mechanism is similar to what has been reported for $[(TPP)Rh^{II}]_2$[39] and $[(Pc)Rh^{II}]_2$[40] where Pc = the dianion of phthalocyanine.

In summary, the electrochemical data for (OMC)Rh(PPh_3) suggest the presence of monomers and dimers in solution and the reduction is proposed to occur according to the overall mechanism given in Scheme II. Scheme IIb is for conditions of high phosphine concentration and fast potential sweep rate while Scheme IIa is for all other conditions.

The propensity of singly reduced $[(OMC)Rh^{II}]^-$ to dimerize as shown in Scheme IIa is due to the presence of a lone pair electron on the Rh(II) ion and is in agreement with the reported dimerization of electrogenerated monomeric rhodium(II) porphyrins and phthalocyanines, none of which have been isolated as other than transient intermediates in solution.[39,41] A dimerization apparently does not occur at high scan rates in PhCN solutions containing excess of PPh_3 (Scheme IIb) where $(OMC)Rh^{III}(PPh_3)$ is reversibly converted to $[(OMC)Rh^{I}(PPh_3)]^{2-}$ via a stepwise two-electron reduction. The electrogenerated $[(OMC)Rh^{I}(PPh_3)]^{2-}$ loses the axial ligand to give $[(OMC)Rh^{I}]^{2-}$, and this species can be reoxidized to give $(OMC)Rh^{III}$ via two consecutive one-electron-transfer processes. This 4-coordinated Rh(III) product is then reconverted to $(OMC)Rh^{III}(PPh_3)$ as shown in the lower pathway of Scheme IIb.

The ratios of cathodic to anodic peak current for processes 4 and 4′ of $(OMC)Rh^{III}(PPh_3)$ in solutions of excess PPh_3 are almost unity at high scan rates (see Figure 12a), but the peak to peak potential separation is larger than expected due to the fact that the reduction and reoxidation follow two separate pathways which differ only by the presence of a bound PPh_3 molecule. A negative shift of the $E_{1/2}$ (or $E°$) for the overall $(OMC)Rh^{III/I}(PPh_3)$ couple is expected to occur when PPh_3 is axially bound, and this is experimentally observed.

Similar cyclic voltammograms are obtained for the reduction of $(OMC)Rh^{III}(PPh_3)$ at low temperature (Figure 3a) or rapid potential scan rate (Figure 1a) in neat solvents or at low scan rates in PhCN containing PPh_3 (Figure 9). Under these conditions a peak due to the oxidation and cleavage of dimeric $[(OMC)Rh^{II}]_2^{2-}$ (process 5) is always observed as shown in Scheme IIa. Different UV–visible spectra of the overall two-electron reduction product of $(OMC)Rh^{III}(PPh_3)$ are obtained depending upon the controlled potential at which the reduction is carried out. The spectrum obtained after reduction at −1.60 V (Figure 7) is assigned as that of doubly reduced $[(OMC)Rh^{I}]^{2-}$ while the spectrum taken during electrolysis at −1.27 V is assigned as corresponding to $[(OMC)Rh^{I}]_2^{4-}$. Similar UV–visible spectra are obtained when the two solutions are reoxidized at −0.10 V. These latter spectra are slightly different from that of the starting Rh(III) derivative and these are assigned to a 4-coordinated $(OMC)Rh^{III}$ species.

The key difference between parts a and b of Scheme II is the lack of a dimerization step under the latter solution conditions. This may be due in part to the fact that the PPh_3 dissociation from $[(OMC)Rh^{II}(PPh_3)]^-$ would be decreased in the presence of excess PPh_3, leaving little or none of the 4-coordinated Rh(II) species to react in solution. This form of the corrole would also not be present in large quantities on the return positive potential scan since, under these conditions, it would be oxidized to give $(OMC)Rh^{III}$ as soon as it was generated at the electrode surface.

In summary, this paper has presented the first detailed electrochemistry for the oxidation and reduction of (OMC)Rh(PPh_3) and (OMC)Co(PPh_3) in nonaqueous media. Up to three well-defined oxidations of the two complexes are observed and this can be contrasted with the porphyrins where only π cation radicals and dications are formed in the absence of a metal-centered reaction. The potentials for generation of $[(OMC)M(PPh_3)]^n$, where M = Rh or Co and n = 1 or 2, are quite negative with respect to values of $E_{1/2}$ for formation of the porphyrin π cation radicals and dications, and it is anticipated that similar facile oxidations should also occur for OMC complexes of Fe(III) and Mn(III). Initial studies on these and other main-group corroles are now in progress.

Acknowledgment. The support of the National Science Foundation (Grant No. CHE-8822881) and National Institute of Health (Grant No. GM-25172) is gratefully acknowledged.

(38) Gutmann, V. *Coord. Chem. Rev.* **1976**, *18*, 225.
(39) Kadish, K. M.; Yao, C.-L.; Anderson, J. E.; Cocolios, P. *Inorg. Chem.* **1985**, *24*, 4515.
(40) Tse, Y.-H.; Seymour, P.; Kobayashi, N.; Lam, H.; Leznoff, C. C.; Lever, A. B. P. *Inorg. Chem.* **1991**, *30*, 4453.
(41) Wayland, B. B.; Newman, A. R. *J. Am. Chem. Soc.* **1979**, *101*, 6472.